Density Functional Description of the Early Stages of the Dioxygenation of [(MeC(CH_2PPh_2)$_3$)M(catecholate)]$^+$ Complexes [M = Co(III), Ir(III)]: Toward a Rationalization of the Catalytic Mechanism of Ring-Opening Dioxygenases

Alessandro Bencini,*,† Eckhard Bill,‡ Fabio Mariotti,§ Federico Totti,† Andrea Scozzafava,† and Angelo Vargas||

Dipartimento di Chimica, Università di Firenze, Firenze, Italy, Max-Planck-Institut für Strahlenchemie, Mülheim, Germany, Departément de Chimie, Université de Fribourg, Fribourg, Switzerland, and Laboratorium für Technische Chemie, ETH Zentrum, Zürich, Switzerland

Received June 2, 1999

Density Functional Theory (DFT) has been applied to characterize the early stages of the reaction of dioxygenation of [(triphos)M(catecholate)]$^+$ complexes [M = Co(III), Ir(III); triphos = MeC(CH_2PPh_2)$_3$], which have been considered to be models of ring-opening dioxygenases. The structural features of the starting complexes and of the intermediate complexes formed by additon of O_2 to the coordinated catecholato ion are well reproduced. The calculations showed that this preliminary stage can be obtained only when the oxygen molecule attacks the molecule on the catecholato site.

Introduction

Catechol is known to be easily oxidized by molecular oxygen to *o*-quinone, but under particular conditions, i.e. when the catechol is bound to a metal center, breaking of the aromatic ring with formation of muconic acid derivatives is observed. This latter reaction is commonly found in the metabolic pathway of aerobic microorganisms, which uses aromatic substances as a carbon source, and it is performed with the help of metalloenzymes referred as ring cleaving dioxygenases.

The active site of these metalloenzymes contains pentacoordinated Fe(III) or Fe(II) ions, which are essential for the catalytic activity, bound to protein ligands (mostly histidines and tyrosines) and water molecules.[1] These dioxygenases can be divided into two classes on the basis of the site of cleavage of the aromatic ring and of the oxidation state of the metal ion. The *extra*diol dioxygenases catalyze the cleavage of the ring adjacent to the vicinal hydroxyl groups and generally contain iron(II) ions.[1,2] The *intra*diol dioxygenases employ iron(III) and open the ring by breaking the carbon−carbon bond between the hydroxyl groups. In both classes the catechol substrate has been proven to bind directly to the metal center.[3,4] More recently, iron(III) complexes that gave *extra*diol cleavage of the catechols have been reported,[5] as well as the structure of a Mn(II)-containing dioxygenase (homoprotocatechuate 2,3-dioxygenase), which catalyzes the *extra*diol cleavage like the iron(II) derivative.[6]

The catalytic mechanisms have been the subject of detailed experimental studies,[7] and the problem of the dioxygen activation is still a matter of debate. While for the iron(II)-containing enzymes it is accepted that direct binding of the dioxygen to the metal center represents the mechanism of oxygen activation, for the iron(III)-containing enzymes a more indirect reaction mechanism has been proposed that involves the electrophilic attack of O_2 to the iron(III)-chelated catecholate moiety.[1−3]

Besides the enzymes, some complexes of the transition metal series have been also found to catalyze the ring breaking of catechol and its derivatives.[8] Furthermore, in one case the putative reaction intermediate between the catecholate metal complex and the dioxygen has been isolated, namely, the complex [(triphos)Ir(O_2)(PhenSQ)]BPh_4 (triphos = MeC(CH_2PPh_2)$_3$; PhenSQ = 9,10-phenanthrenesemiquinonate), and its molecular structure solved by X-ray diffraction methods.[8i] The structure of this complex is shown in Chart 1, together with the most relevant geometrical parameters. The dioxygen is

† Università di Firenze.
‡ Max-Planck-Institut für Strahlenchemie.
§ Université de Fribourg.
|| Laboratorium für Technische Chemie.

(1) (a) Lipscomb, J. D.; Orville, A. M. In *Metal Ions in Biological Systems*; Siegel, H., Siegel, A., Eds.; Marcel Dekker: New York, 1992; Vol. 28. (b) Que, L., Jr.; Ho, R. Y. N. *Chem. Rev.* **1996**, *96*, 2607. (c) Bertini, I.; Briganti, F.; Mangani, S.; Nolting, H. F.; Scozzafava, A. *Coord. Chem. Rev.* **1995**, *144*, 321.
(2) Que, L., Jr.; Dong, Y. *Acc. Chem. Res.* **1996**, *29*, 190.
(3) Orville, A. M.; Lipscomb, J. D.; Ohlendorf, D. H. *Biochemistry* **1997**, *36*, 10052.
(4) Stenkamp, R. E. *Chem. Rev.* **1994**, *94*, 715.
(5) Jo, D.-H.; Que, L., Jr. *J. Inorg. Biochem.* **1999**, *74*, 180. Paper presented at the 9th International Conference on Biological Inorganic Chemistry, Minneapolis, July 11−16, 1999.
(6) Vetting, M. W.; Que, L., Jr.; Lipscomb, J. D.; Ohlendorf, D. H. *J. Inorg. Biochem.* **1999**, *74*, 179. Paper presented at the 9th International Conference on Biological Inorganic Chemistry, Minneapolis, July 11−16, 1999.
(7) (a) Arciero, D. M.; Lipscomb, J. D. *J. Biol. Chem.* **1986**, *261*, 2170. (b) Mabrouk, P. M.; Orville, A. M.; Lipscomb, J. D.; Solomon, E. I. *J. Am. Chem. Soc.* **1991**, *113*, 4053. (c) Shu, L.; Chiou, Y.-M.; Orville, A. M.; Miller, M. A.; Lipscomb, J. D.; Que, L., Jr. *Biochemistry* **1995**, *34*, 6649. (d) Fujisawa, H.; Hiromi, K.; Uyeda, M.; Nozaki, M.; Hayaishi, O. *J. Biol. Chem.* **1971**, *246*, 2320. (e) Fujisawa, H.; Hiromi, K.; Uyeda, M.; Okuno, S.; Nozaki, M.; Hayaishi, O. *J. Biol. Chem.* **1972**, *247*, 4422. (f) Que, L., Jr.; Lipscomb, J. D.; Zimmermann, R.; Münck, E.; Orme-Johnson, N. R.; Orme-Johnson, W. H. *Biochim. Biophys. Acta* **1976**, *452*, 320. (g) Bull, C.; Ballou, D. P.; Otsuka, S. *J. Biol. Chem.* **1981**, *256*, 12681. (h) May, S. W.; Oldham, C. D.; Mueller, P. W.; Padgette, S. R.; Sowell, A. L. *J. Biol. Chem.* **1982**, *257*, 12746. (i) Witthaker, J. W.; Lipscomb, J. D. *J. Biol. Chem.* **1984**, *259*, 4476; **1984**, *259*, 4487. (j) Witthaker, J. W.; Lipscomb, J. D.; Kent, T. A.; Münck, E. *J. Biol. Chem.* **1984**, *259*, 4466.

10.1021/ic990633i CCC: $19.00 © 2000 American Chemical Society
Published on Web 03/16/2000

Chart 1

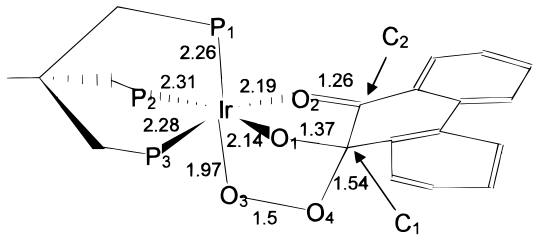

bound to the iridium(III) center and was found to be disordered over the two carbon atoms of the semiquinonato ligand. Nevertheless, it is bound to one carbon, which acquires some sp^3 character breaking the aromaticity of the ring.

This reaction intermediate of Chart 1 looks very similar to the intermediate proposed in the qualitative reaction scheme used to rationalize the catalytic activity of the enzymes. According to the mechanism proposed by Que et al.,[9] the reaction of such Fe(III) enzymes proceeds by the activation of the cathecolate moiety after coordination to the acidic Fe(III) center and subsequent quinonization and formation of a peroxide bridge with the incoming oxygen molecule. This mechanism has received some justification by orbital interaction considerations at the extended Hückel level of calculation,[10] and more recently, a linear correlation between the natural logarithm of the kinetic constants of the various steps of the reaction and the energies of the HOMO of various substrates computed at the AM1 level was established.[11] This correlation adds to the well-known correlations established by Que et al. showing that the rate of oxygenation in several model systems increases with decreasing energy of the electronic transition occurring in the visible region of the spectra, assigned to a catecholato-to-iron(III) charge-transfer transition.[8a]

Since the exact nature of the transition metal does not seem to play a key role in the mechanism of action of the dioxygenases[5,6] and since experimental structures are available, we decided to approach the theoretical study of the dioxygenase reactions by applying quantum mechanical techniques to the characterization of the reactions of the above-mentioned complexes of Co(III) and Ir(III). These complexes, in contrast to the iron systems, are diamagnetic, and the calculations do not have to take into account the multiplet structure of the systems, which would be a considerable theoretical task[12] and would influence the accuracy of the results. The present study cannot, therefore, give direct information about the role of the enzymatic environment in the reaction, but it should be considered as a test of the quantum mechanical techniques applied to complex molecular systems and as a preliminary step for further calculations. We have applied density functional theory (DFT) to characterize the preliminary stages of the reaction between the [(triphos)M(catecholate)] $^+$ (M = Co, Rh, Ir) and dioxygen, using several different catecholates and M = Co and Ir. These reactions are spin-forbidden, since the final complexes are all diamagnetic and since no paramagnetic intermediate was experimentally observed that can support the transfer of the spin from the oxygen, which in the ground state is in a triplet state. The spin−orbit coupling, which mixes triplet and singlet states, seems to be the most probable mechanism that allows the reaction. Because of the intrinsic difficulty of DFT for treating multiplets, which requires multideterminant wave functions, and because of the complexity of including spin−orbit coupling effects at a reasonable level of accuracy, a complete study of the potential energy surface (PES) of the reaction was not attempted. Rather, we have explored some important points of this surface by geometry optimizations of the set [(triphos)M-(catecholate)]$^+$ + O_2, arranging the oxygen molecule in different spatial positions with respect to the metal. The calculations were performed using two computer programs, namely, the Amsterdam Density Functional (ADF) program[13] and Gaussian 98.[14] The first program uses Slater type orbitals and is widely used to handle spectroscopic properties of transition metal complexes. The second program package includes semiempirical, HF, and post-HF methods as well as density functionals and is one of the most used quantum chemical program packages. Some comparison between the results obtained by the two programs is drawn in Conclusions.

Computational Details

All the calculations have been performed using the Amsterdam Density Functional (ADF)[13] and the Gaussian 98[14] program packages.

ADF calculations were performed using the Xα functional[15] for the exchange and the Vosko, Wilk, and Nusair functional[16] for the correlation potential. This form of functional is also known as LSDA (local spin density approximation). The Stoll correlation correction[17] for the electrons with the same spin was also included in the

(8) (a) Cox, D. D.; Que, L., Jr. *J. Am. Chem. Soc.* **1988**, *110*, 8085. (b) Cox, D. D.; Benckovic, S. J.; Bloom, L. M.; Bradley, F. C.; Nelson, M. J.; Que, L., Jr.; Wallick, D. E. *J. Am. Chem. Soc.* **1988**, *110*, 2026. (c) Jang, H. G.; Cox, D. D.; Que, L., Jr. *J. Am. Chem. Soc.* **1991**, *113*, 9200. (d) Weller, M. G.; Weser, U. *J. Am. Chem. Soc.* **1982**, *104*, 3752. (e) Weller, M. G.; Weser, U. *Inorg. Chim. Acta* **1985**, *107*, 243. (f) Funabiki, T.; Mizoguchi, A.; Sugimoto, T.; Tada, S.; Tsuji, M.; Sakamoto, H.; Yoshida, S. *J. Am. Chem. Soc.* **1986**, *108*, 2921. (g) Funabiki, T.; Konishi, T.; Kobayashi, S.; Mizoguchi, A.; Takano, M.; Yoshida, S. *Chem. Lett.* **1987**, 719. (h) Que, L., Jr.; Kolanczyk, R. C.; White, L. S. *J. Am. Chem. Soc.* **1987**, *109*, 5373. (i) Barbaro, P.; Bianchini, C.; Linn, K.; Mealli, C.; Meli, A.; Vizza, F. *Inorg. Chim. Acta* **1992**, *198*−*200*, 31. (j) Dei, A.; Gatteschi, D.; Pardi, L. *Inorg. Chem.* **1993**, *32*, 1389. (k) Barbaro P.; Bianchini, C.; Frediani, P.; Meli, A.; Vizza, F. *Inorg. Chem.* **1992**, *31*, 1523.

(9) Que, L., Jr.; Lipscomb, J. D.; Münck, E.; Wood, J. M. *Biochim. Biophys. Acta* **1977**, *485*, 60.

(10) Funabiki, T.; Inque, T.; Kojima, H.; Konishi, T.; Tanaka, T.; Yoshida, S. *J. Mol. Catal.* **1990**, *59*, 367.

(11) Ridder, L.; Briganti, F.; Boersma, M. G.; Vis, H, E.; Scozzafava, A.; Veeger, C.; Rietjens, I. M. C. M *Eur. J. Biochem.* **1998**, *257*, 92.

(12) Daul, C. A.; Doclo, K.; Stukl, A. C. In *Recent Advances in Density Functional Methods*; Chong, D. P., Ed.; World Scientific: Singapore, 1997; Part II, p 61.

(13) (a) *Amsterdam Density Functional (ADF)*, revision 2.3; Scientific Computing and Modelling, Theoretical Chemistry, Vrije Universiteit: Amsterdam, 1997. (b) Baerends, E. J.; Ellis, D. E.; Ros, P. *Chem. Phys.* **1973**, *2*, 42. (c) Boerrigter, P. M.; te Velde, G.; Baerends, E. J. *Int. J. Quantum Chem.* **1988**, *33*, 87. (d) te velde, G.; Baerends, E. J. *J. Comput. Phys.* **1992**, *99*, 84. (e) Fonseca Guerra, C.; Visser, O.; Snijders, J. G.; te Velde, G.; Baerends, E. J. In *Methods and Techniques in Computational Chemistry*; Clementi, E., Corongiu, C., Eds.; STEF: Cagliari, Italy, 1995; Chapter 8, p 305.

(14) Frisch, M. J.; Trucks, G. W.; Schlegel, H. B.; Scuseria, G. E.; Robb, M. A.; Cheeseman, J. R.; Zakrzewski, V. G.; Montgomery, J. A., Jr.; Stratmann, R. E.; Burant, J. C.; Dapprich, S.; Millam, J. M.; Daniels, A. D.; Kudin, K. N.; Strain, M. C.; Farkas, O.; Tomasi, J.; Barone, V.; Cossi, M.; Cammi, R.; Mennucci, B.; Pomelli, C.; Adamo, C.; Clifford, S.; Ochterski, J.; Petersson, G. A.; Ayala, P. Y.; Cui, Q.; Morokuma, K.; Malick, D. K.; Rabuck, A. D.; Raghavachari, K.; Foresman, J. B.; Cioslowski, J.; Ortiz, J. V.; Stefanov, B. B.; Liu, G.; Liashenko, A.; Piskorz, P.; Komaromi, I.; Gomperts, R.; Martin, R. L.; Fox, D. J.; Keith, T.; Al-Laham, M. A.; Peng, C. Y.; Nanayakkara, A.; Gonzalez, C.; Challacombe, M.; Gill, P. M. W.; Johnson, B. G.; Chen, W.; Wong, M. W.; Andres, J. L.; Head-Gordon, M.; Replogle, E. S.; Pople, J. A. *Gaussian 98*, revision A.5; Gaussian, Inc.: Pittsburgh, PA, 1998.

(15) Slater, J. C. *Quantum Theory of Molecules and Solids. Vol. 4: Self-Consistent Field for Molecules and Solids*; McGraw-Hill: New York, 1974.

(16) Vosko, S. H.; Wilk, L.; Nusair, M. *Can. J. Phys.* **1980**, *58*, 1200.

(17) Stoll, H.; Pavlidou, C. M. E.; Preuss, H. *Theor. Chim. Acta* **1978**, *49*, 143.

calculations. The frozen core (FC) approximation for the inner core electrons was used. The orbitals up to 3p for cobalt, 5p for iridium, 2p for phosphorus, and 1s for oxygen and carbon were kept frozen. Valence electrons on each atom were treated with triple-ζ basis functions except hydrogens, which were treated with a single-ζ function. The valence shells of non-hydrogen atoms were expanded with single-ζ p polarization functions for Co and Ir and with single-ζ d polarization functions for C, O, and P. The exponents of the Slater functions given with the ADF2.3 distribution were used throughout. Electronic transitions were computed by applying Slater's transition-state theory.[15]

In the calculations performed with Gaussian 98 we used both LSDA and GGA approximations. The GGA calculations were performed using the Perdew−Wang exchange−correlation functional.[18] The LANL2DZ relativistic effective core potentials[19] and the basis set for the metals and P were used. To C and H the D95(d) basis was applied.[20]

The triphos ligand $MeC(CH_2PPh_2)_3$ was replaced in all the calculations by the simpler model ligand triphosH, $HC(CH_2PH_2)_3$, in which the phenyl rings and the methyl group of the phosphine were replaced by H atoms. All the complexes studied belong to the C_1 point symmetry group. Geometry optimizations were performed in Cartesian coordinates. Frequencies were computed in order to completely characterize the computed structure of the adducts with dioxygen. In ADF a numerical differentiation of energy gradients in slightly displaced geometries was used,[21] while analytic second derivatives were available in Gaussian 98. The numerical derivatives were computed using only one displacement for each atomic coordinate, the calculation requiring 106 gradients for the evaluation. This procedure, although less accurate than the standard one requiring two displacements for each atomic coordinate, was used to save computer time, which became prohibitive for the large molecules we handled. More accurate calculations were also performed on the iridium complex using double displacements and higher integration accuracy (INT = 8 instead of 6).

Calculations on the iridium complexes were performed, which included the scalar relativistic corrections, Darwin and mass−velocity, in the quasi-relativistic approach implemented in ADF.[22]

Results and Discussions

Geometric and Electronic Structure. The structure of the $[(triphosH)Co(catecholato)]^+$ cation computed by geometry optimization with ADF is shown in Figure 1a. The relevant geometrical parameters are also compared, in Figure 1a, to the experimental values found for the crystal structure of $[(triphos)Co(III)(catecholato)]BF_4 \cdot CH_2Cl_2$.[23] The agreement between the two structures is apparent, indicating that the chosen functional and basis can give a correct description of the structural features of the complex. The experimental compound shows some differences between the two nonequivalent C−O distances, namely, 1.36 vs 1.32 Å, which cannot be reproduced by the calculations, which always give 1.32 Å. In Figure 1b the computed structure of the analogous Ir derivative is shown. Calculations on the iridium complexes were performed using the quasi-relativistic approach[22] because of the large mass of the iridium atom. Since no structure is available for the Ir complex, a direct comparison of the results is not possible. The computed energy levels near the HOMO−LUMO region are shown in Figure 2, where the computed lower energy transitions

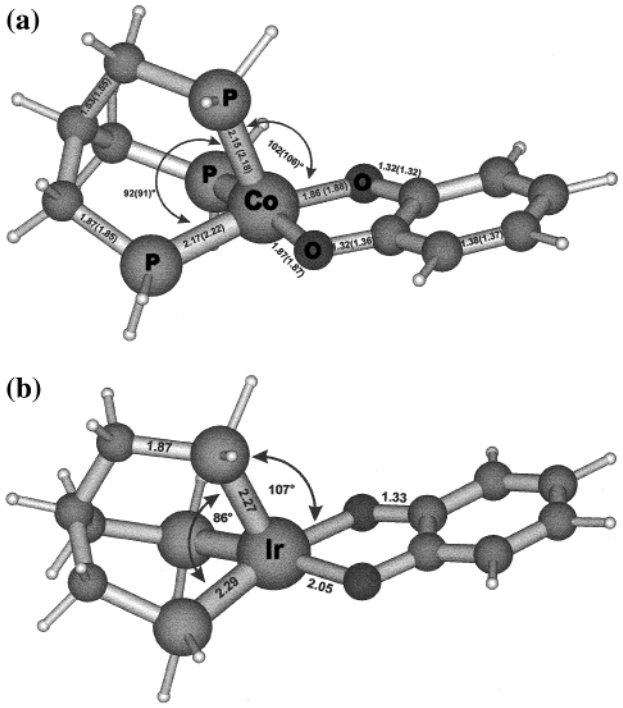

Figure 1. (a) Optimized structure (ADF-LSDA) of the $[(triphosH)Co(catecholato)]^+$ cation. Relevant bond distances (Å) and angles (deg) are shown. The values in parentheses are the experimental results. When only one value is reported for nonequivalent bonds and angles, it refers to the average over the nonequivalent data. (b) Optimized structure (ADF-LSDA) of the $[(triphosH)Ir(catecholato)]^+$ cation. Nonmetallic atoms are labeled as in part a.

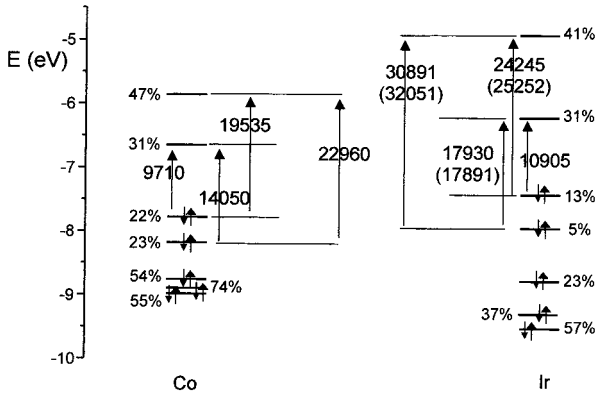

Figure 2. Computed energy levels (ADF-LSDA) near the HOMO−LUMO region for $[(triphosH)Co(catecholato)]^+$ and $[(triphosH)Ir(catecholato)]^+$. The metal d contribution is indicated as a percentage of the gross atomic orbital population. The computed one-electron transition energies between the levels indicated by the arrows are shown. Experimental values are reported in parentheses.

are also indicated. The spectra are characterized by four transitions in the UV−vis region. For the iridium derivative, the transitions observed in the 4-methylcatecholate complex, are shown in Figure 2 in parentheses. The agreement with the computed transitions is apparent. No spectral data have been reported for the analogous complex of cobalt(III). In the parent complex with the di-*tert*-butylcatecholate ligand, transitions at 12 400 cm^{-1}, 16 300, 23 260, and 26 740 cm^{-1} were reported. These transition were experimentally assigned[8i] to ligand-to-metal charge transfer (LMCT) transitions because of their intensities ($e_M \approx 2000-5000$ cm^{-1} mol^{-1}). In all cases, spectral data below 11 000 cm^{-1} were not available. A pictorial representation of the HOMO − 1, HOMO, LUMO, and LUMO

(18) Burke, K.; Perdew, J. P.; Wang, Y. In *Electronic Density Functional Theory: Recent Progress and New Directions*; Dobson, J. F., Vignale, G., Das, M. P., Eds.; Plenum Press: New York, 1998.
(19) (a) Hay, P. J.; Wadt, W. R. *J. Chem. Phys.* **1985**, *82*, 270. (b) Wadt, W. R.; Hay, P. J. *J. Chem. Phys.* **1985**, *82*, 284. (c) Hay, P. J.; Wadt, W. R. *J. Chem. Phys.* **1985**, *82*, 299.
(20) Dunning, T. H.; Hay, P. *Modern Theoretical Chemistry*; Schaefer, H. F., Ed.; Plenum: New York, 1976.
(21) (a) Fan, L.; Ziegler, T. *J. Phys. Chem.* **1992**, *96*, 6937. (b) Fan, L.; Ziegler, T. *J. Chem. Phys.* **1992**, *96*, 9005.
(22) Ziegler, T.; Tschinke, V.; Baerends, E. J. *J. Phys. Chem.* **1989**, *93*, 3050.
(23) Vogel, S.; Huttner, G.; Zsolnai, L. *Z. Naturforsch., B* **1993**, *48*, 641.

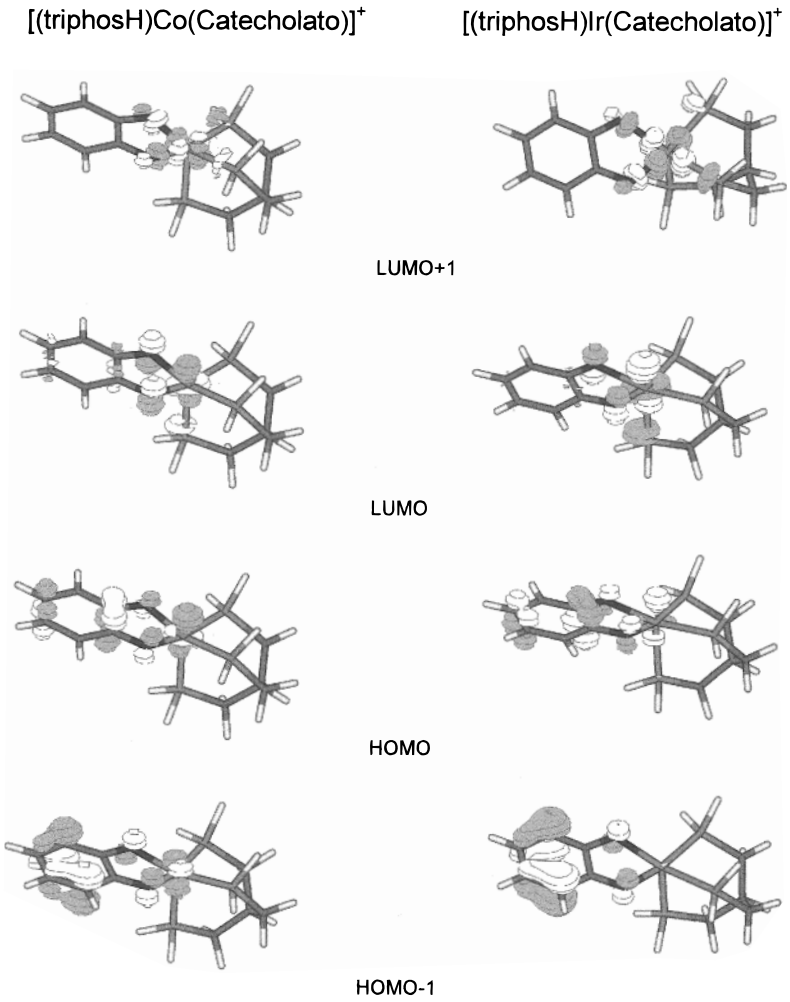

Figure 3. Frontier orbitals (ADF-LSDA) of [(triphosH)Co(catecholato)]$^+$ (left) and [(triphosH)Ir(catecholato)]$^+$ (right) represented as isovalue surfaces ($\psi = 0.07$ au). Positive values of the wave function are represented in white.

+ 1 orbitals of the [(triphosH)Co(catecholato)]$^+$ and [(triphosH)-Ir(catecholato)]$^+$ complexes is given in Figure 3. The classification of the molecular orbitals is difficult because of the absence of symmetry of the complex, which causes mixing of many different atomic orbitals. In Figure 2, the contribution to the molecular orbitals from the d orbitals of the metal is shown as a percentage of the gross atomic orbital population, obtained by Mulliken analysis. In a rough classification, which neglects low-symmetry effects, we can divide the d metal orbitals such as in an octahedral complex into a set of three π orbitals and two σ orbitals. If we choose the plane containing the two P atoms of the triphos, the two oxygens and the metal as the *xy* plane, the π orbitals are in-plane, *xy*, and out-of-plane, *xz* and *yz*. The σ orbitals are largely destabilized by the interaction with the phosphine, the in-plane, $x^2 - y^2$, being at higher energy with respect to the axial, z^2, orbital. The *xy* orbital is expected to be roughly nonbonding, since it lies in a nodal plane of the catecholato ligand, which is the only ligand that can give significant π interaction. The three levels at lower energy in Figure 3 have a large metal-d character, which decreases on passing to the iridium(III) complex, and can be assigned to the three π-type orbitals, the in-plane one being at the lowest energy and more centered onto the metal. The next MO (HOMO − 1) is mainly localized on the catecholate ion with a small antibonding contribution from one of the π out-of-plane d orbitals. The metal contribution is lowered to be only 5% in the iridium(III) complex. HOMO and LUMO are composed of σ-axial metal orbitals largely delocalized over the aromatic ring, with the LUMO having more metallic character. The LUMO + 1 orbital is easily assigned to an in-plane $x^2 - y^2$ like orbital, with metal-P and metal-O σ-antibonding character.

To find the preferred site of attack of dioxygen on the substrate, we performed a series of geometrical optimization of the system [(triphosH)Co(catecholate)]$^+$ + O_2 varying the relative position of O_2 with respect to the complex. In all cases, two minima were found: one corresponding to a complex in which O_2 binds to the Co(III) center; the other one to a complex in which the oxygen bridges the Co and the carbons of the aromatic ring. This latter situation is always met when we allow the O_2 molecule to approach the complex from the carbon side. The geometries of these two complexes are shown in Figure 4, where the relevant geometrical parameters are also reported. Comparison of the computed bond lengths for the dioxygen bridged complex with the experimental values reported in Chart 1 shows very nice agreement irrespective of the nature of the metal (Co in the calculation, Ir in the experimental structure). The structure of the analogous iridium complex, [(triphosH)-Ir(O_2)(catecholato)]$^+$, optimized using the quasi-relativistic approach[22] because of the large mass of the iridium atom, is shown in Figure 5, together with the computed relevant geometrical parameters. The agreement with the observed structure (Chart 1) is rather good. The largest deviation (6%) is in the computed Ir−O_2 bond distance: 2.09 vs 1.97 Å. However,

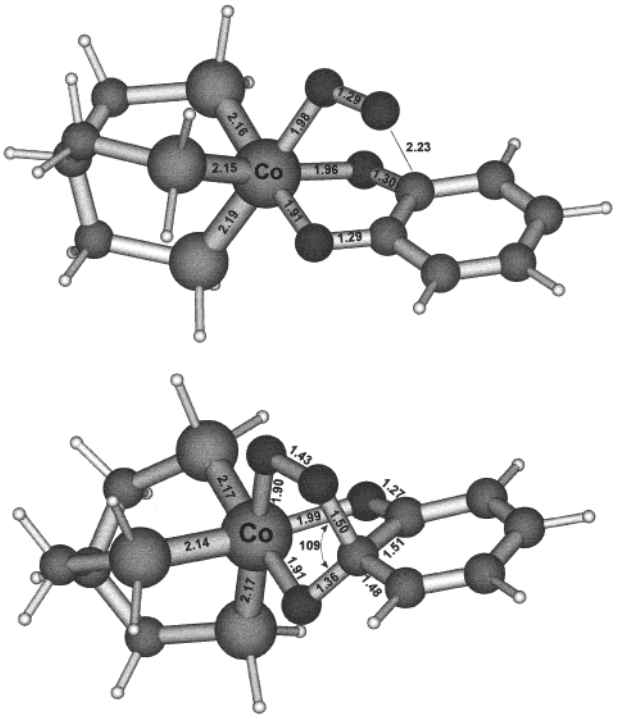

Figure 4. Computed structures (ADF-LSDA) for the two possible adducts of O_2 to [(triphosH)Co(catecholato)]$^+$. Relevant bond distances (Å) and angles (deg) are shown. Nonmetallic atoms are labeled as in Figure 1a.

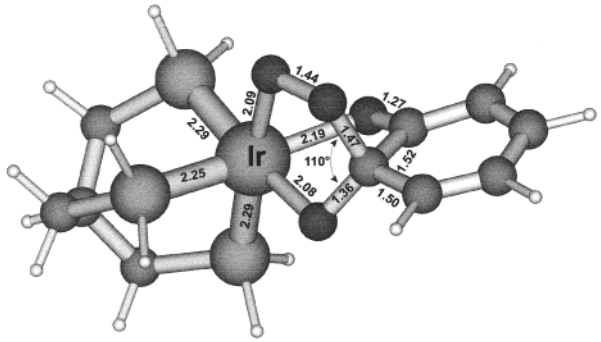

Figure 5. Computed structure (ADF-LSDA) [(triphosH)Ir(O_2)-(catecholato)]$^+$. Relevant bond distances (Å) and angles (deg) are shown. Reference experimental data are shown in Chart 1. Nonmetallic atoms are labeled as in Figure 1a.

the experimental value of this distance reflects the disorder of the dioxygen observed in the experimental structure.

The computed structures of [(triphosH)Ir(catecholato)]$^+$, [(triphosH)Ir(O_2)(catecholato)]$^+$, [(triphosH)Ir(catecholato)]$^+$, and [(triphosH)Co(O_2)(catecholato)]$^+$ have been further characterized by computing the vibrational frequencies as described in Computational Details. This is required in order to distinguish, among the stationary points of the potential surface, between relative minima, maxima, and transition states.[24] In all cases, three eigenvalues of the computed Hessian matrix were found to be imaginary when ADF was used in the calculations. This should not correspond to any chemically meaningful point of the potential surface describing the nuclear rearrangement of the reagents. However, a careful examination of these imaginary vibrations shows that they can be due to an incomplete subtraction of the translational and rotational modes of the molecules due to the computational approximations required for computing numerically the Hessian matrix using reasonable computer time. These imaginary solutions were also computed in the deoxygenated complex [(triphosH)Ir(catecholato)]$^+$ where the structure must belong to a minimum energy configuration. Another source of error in the calculation of the vibrational modes is the uncertainty in the location of the stationary points, which for such large systems is always affected by some errors.

Complete geometrical optimizations have also been performed using Gaussian 98 in the LSDA approximations. The relevant geometrical parameters computed with ADF and Gaussian 98 are compared in Table 1. It is apparent that there is overall agreement between the structures computed with the two methods. The IR vibrational frequencies obtained with this latter program were, however, all positive. This result is due to the analytical procedure of Gaussian 98, which appears to be more accurate for these systems. The computed IR vibrational frequencies corresponding to mainly C−O and C═C stretches are collected in Table 2 and compared with the experimental results. The frequencies computed, with ADF, for the free ligands are also reported. The frequencies reported as a C−O stretch are strongly admixed with C−C vibrations in all cases. The ν(C−O) computed for [(triphosH)Ir(catecholato)]$^+$ are between those computed for catecholato and semiquinonato but nearer the catecholato limit. The values reported in Table 2 for the free ligands correspond to the symmetric (lower energy) and antisymmetric stretch of the two C−O groups. Upon coordination of dioxygen, two sets of frequencies involving the C−O groups are computed. The frequencies at lower energy correspond to motions involving the C−O group to which the dioxygen is coordinated, in agreement with experimental results. It should be noted that the vibrational frequencies computed by both ADF and Gaussian 98 compare well with each other and are in nice agreement with the experimental findings. Therefore, even if the low-energy region of the spectrum is not correctly taken into account with the ADF calculations, chemically significant vibrations are reproduced.

The overall agreement with the experimental results can be considered satisfactory. Therefore, the computed structure can be considered a good representation of the real complexes, confirming the ability of DFT to represent the structure and properties of complex molecular systems.

Some Energetic Considerations. The relative stability of the complexes can be computed from the enthalpy of the reaction

$$[(\text{triphosH})\text{M}(\text{catecholato})]^+ + \text{O}_2 \leftrightarrows [(\text{triphosH})\text{M}(\text{O}_2)(\text{catecholato})]^+$$

In doing these calculations, we used the oxygen in the ground triplet state with the energy computed on the optimized geometry at the appropriate level of approximation. Using LSDA, we obtained ΔH_r(Co) = −19.25 (−30.33) kcal mol^{-1} and ΔH_r(Ir) = −24.46 (−35.08) kcal mol^{-1}. The values in parentheses were computed with Gaussian 98. These computed values are largely affected by the energy of the oxygen molecule. By allowance for the reaction of oxygen in the singlet state and by use of the experimental transition energy of 22.64 kcal mol^{-1} for the singlet−triplet ($^1\Delta_g$−$^3\Sigma_g^-$) separation in O_2, the relative stability of the oxygenated adduct decreases. The computed values are ΔH_r(Co) = 3.39 (−7.59) kcal mol^{-1} and ΔH_r(Ir) = −1.82 (−12.44) kcal mol^{-1}, indicating that the accurate evaluation of the energy of dioxygen is important for meaningful evaluation of the reaction enthalpy. This quantity does not influence the relative stability of the dioxygen Co and Ir complexes, which

(24) Salem, L. *Electrons in Chemical Reactions*; John Wiley & Sons: New York, 1982.

Table 1. Comparison between Relevant Geometrical Parameters Computed with ADF and Gaussian 98 for the Co and Ir Catecholates Complexes[a]

	[(triphosH)Co (catecholato)]$^+$	[(triphosH)Co(O_2) (catecholato)]$^+$	[(triphosH)Ir (catecholato)]$^+$	[(triphosH)Ir(O_2) (catecholato)]$^+$
$M-P_1$	2.15 (2.18)	2.17 (2.19)	2.27 (2.31)	2.29 (2.33)
$M-P_2$	2.17 (2.20)	2.17 (2.19)	2.29 (2.33)	2.29 (2.33)
$M-P_3$	2.17 (2.20)	2.14 (2.16)	2.29 (2.33)	2.25 (2.29)
$M-O_1$	1.86 (1.83)	1.91 (1.88)	2.05 (2.00)	2.08 (2.04)
$M-O_2$	1.87 (1.83)	1.99 (1.94)	2.04 (1.99)	2.19 (2.10)
$M-O_3$		1.90 (1.88)		2.09 (2.04)
$C-O_4$		1.50 (1.54)		1.47 (1.50)
O_3-O_4		1.43 (1.47)		1.44 (1.50)
C_1-O_1	1.32 (1.35)	1.36 (1.39)	1.33 (1.36)	1.36 (1.41)
C_2-O_2	1.32 (1.35)	1.27 (1.30)	1.33 (1.36)	1.27 (1.30)
$O_4-C_1-O_1$		109 (107)		110 (109)
O_1-M-P_1	102 (103)	93 (91)	107 (105)	95 (93)

[a] Bond distances are in Å, angles in deg. The atoms are numbered in Chart 1. Gaussian 98 results are reported in parentheses.

Table 2. Comparison between Computed Vibrational Frequencies (cm^{-1}) for the Free and Coordinated Catecholates[a]

compound	ν(C−O)	ν(C−C)
catecholato	1291 (70)	1064 (12)
d(C−O) = 1.348 Å	1415 (34)	1377 (70)
		1524 (50)
semiquinonato	1597 (315)	1007 (13)
d(C−O) = 1.249 Å	1605 (113)	1094 (19)
		1536 (104)
		1557 (11)
quinone	1717 (177)	1117 (15)
d(C−O) = 1.214 Å	1749 (49)	1121 (10)
		1255 (33)
		1399 (39)

compound	ADF	G98	ADF	G98	expt[b]
[(triphosH)Ir(catecholato)]$^+$	1236 (17)	1273 (12)	1556 (70)	1587 (74)	1262
					1557
[(triphosH)Co(catecholato)]$^+$	1270 (23)	1290 (15)	1590 (82)	1578 (86)	1224
					1580
[(triphosH)Ir(O_2)(catecholato)]$^+$	1158 (64)[c]	1064 (26)[c]	1637 (18)	1655 (42)	1164
	1187 (37)[c]	1142 (25)[c]			1553
	1523 (130)	1503 (197)			1570
	1564 (28)	1570 (24)			1619
[(triphosH)Co(O_2)(catecholato)]$^+$	1160 (56)[c]	1087 (20)[c]	1395 (22)	1172 (18)	
	1183 (13)[c]	1143 (23)[c]	1615 (11)	1648 (27)	
	1480 (103)	1506 (138)			

[a] Only the most intense transitions in the range 1000−4000 cm^{-1} are shown. Absorption intensity km mol^{-1} is given in parentheses. The assignment refers to the main component of the normal coordinate. [b] Values averaged over different compunds. [c] Stretching frequency associated with the long C−O bond.

can be obtained by subtracting the above reaction enthalpies. In this way we computed the iridium(III) adduct to be more stable than the cobalt(III) complex by 5.21 (4.75) kcal mol^{-1}. Using accurate frequency calculations of Gaussian 98, we evaluated the thermodynamic correction to the total energy and computed, taking the oxygen in the ground state, the free energy variations as $\Delta G_r(298K) = -14.9$ and -22.4 kcal mol^{-1} for the Co and Ir derivatives, respectively. The iridium complex is more stable by 7.5 kcal mol^{-1}.

More accurate values of the total energies generally can be computed using the GGA instead of the LSDA, while the latter is known to give better geometries. Using Gaussian 98, we have computed $\Delta H_r(Co) = -10.09$ kcal mol^{-1} and $\Delta H_r(Ir) = -16.09$ kcal mol^{-1} with the iridium complex 6.00 kcal mol^{-1} more stable than the cobalt(III) complex.

The values of ΔH_r and ΔG_r computed with ADF and Gausian 98 are close to each other and show that the iridium adduct is more stable than the cobalt adduct. This is in agreement with the experimental finding that only the iridium complex was isolated and, if this intermediate adducts plays an important role in the dioxygenation reaction, can rationalize the smaller reactivity of the cobalt complexes.

Some Qualitative Considerations. The dioxygenation reactions in the [(triphos)M(L)]$^+$ series was found to depend not only on the nature of the metal center but also on the nature of the ligand L. To look at the effect of the substrate, we have computed the electronic structure of a series of cobalt(III) complexes with different L ligands. The formulas of the ligand used are shown in Figure 6 together with the charge distribution obtained by a Mulliken population analysis. The computed HOMO−LUMO transitions are reported in Table 3 and compared with those of the free ligands.

Since the coordination by the metal does not significantly alter the geometry of the ligand with respect to the free ligand, except the C−O bonds, and because of the qualitative nature of these results, we performed partial geometry optimizations by freezing the metal coordination site with the geometrical parameters obtained by the quantum mechanical calculations of the catecholato adduct of cobalt(III), and optimizing the organic part using standard molecular mechanics techniques

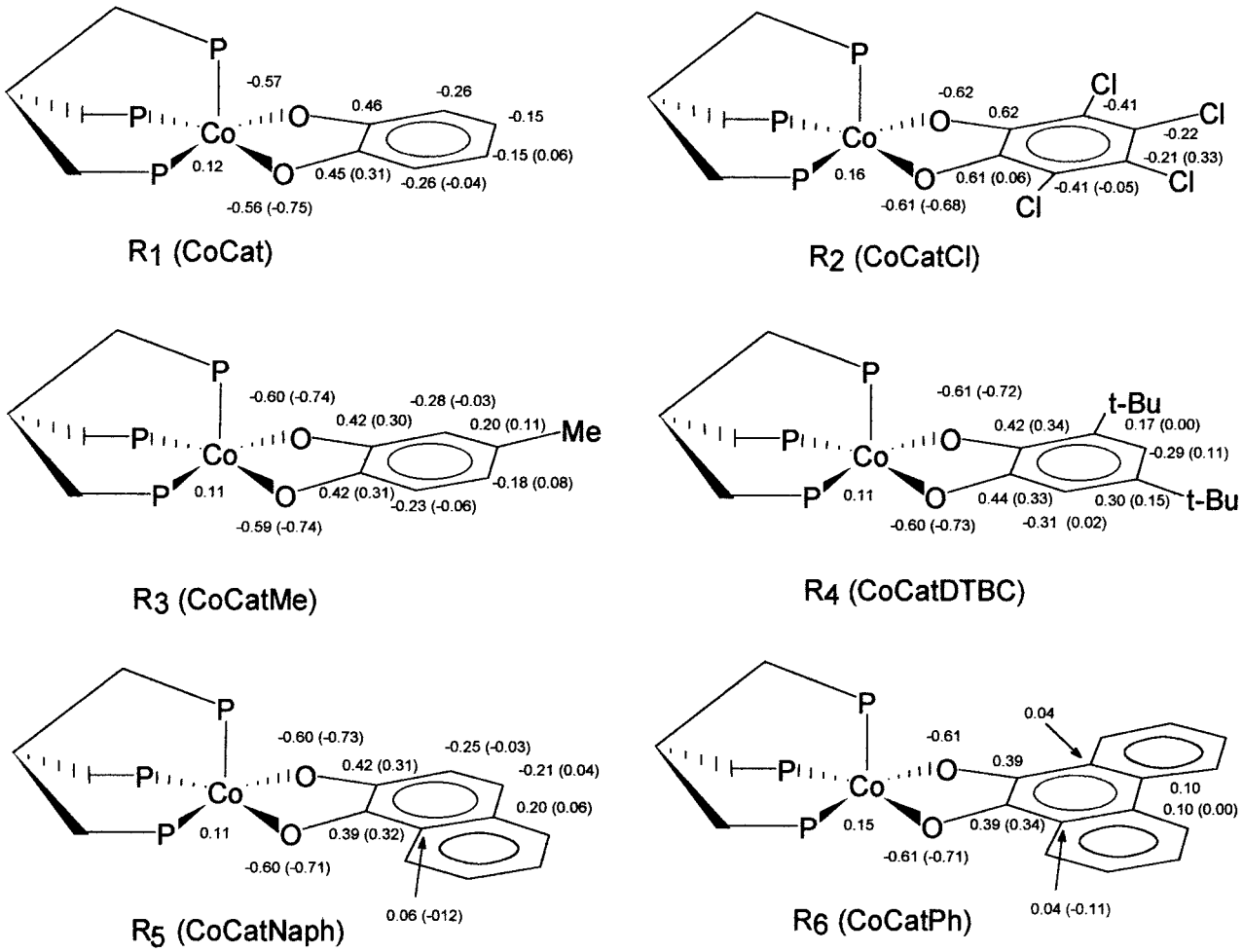

Figure 6. Net charges computed (ADF-LSDA) for a series of cobalt(III)−catecholato complexes. Values in parentheses refer to the charges computed on the free ligands.

Table 3. HOMO−LUMO Energies (cm^{-1}) Computed for the Complexes R_1−R_6 and for the Free Ligands

	R_1	R_2	R_3	R_4	R_5	R_6
Complexes with Ligands						
HOMO−LUMO	9710	9630	9888	9904	8840	8614
Free Ligands						
HOMO−LUMO	25987	17163	23156	20123	12009	8606

(MMP),[25] which is known to perfectly reproduce the geometrical features of organic compounds and to significantly reduce the computer time needed for the calculations.

The computed charge distributions are shown in Figure 6, where they are compared with the charges computed on the free ligand (values in parentheses). We can see that there is a large redistribution of the charges upon coordination, while the charges on the metal center, the oxygen atoms, and the carbon atoms bound to the oxygens do not strongly depend on the substituents on the aromatic ring. The largest variation is observed for the charges on the carbon atoms bound to the oxygens, C_1 and C_2, which vary from an average of 0.42 au for R_1 and R_3−R_6 to 0.62 au for R_2. For the series of complexes shown in Figure 6, since the reactivity was found to follow the series R6 > R4 > R3 ≫ R2, we can see that this trend follows this accumulation of charge: less positive charges being computed for the more reactive species. In fact, the 3,4,5,6-tetrachlorocatechol was found to be unreactive, and it possesses the largest positive charge. These findings also agree with a electrophilic attack of the oxygen on the aromatic ring.

Another quantity that is often monitored to qualitatively follow the reactivity of substrates is the HOMO−LUMO energy difference.[24] From the transition energies reported in Table 3, it can be seen that upon coordination the transition energies shift from the UV to the visible region of the spectra, in agreement with the central role played by the ligand in activating the dioxygenation reaction. A less evident relationship exists between the reactivity of the substrate and the HOMO−LUMO gap. We can only see that the more reactive species, R_6, has the smaller gap. The same qualitative trend is observed in the free ligands, even if the nature of the orbital involved in the transition is completely changed. These findings can strengthen the correlations established in reference 11, which were based on calculations on the free ligands.

Conclusions

DFT has been of valuable help in characterizing the intermediate of the reaction between $[(triphos)M(catecholate)]^+$ and O_2 (M = Co, Ir). Although the spin-forbidden nature of the reaction, which can be allowed by spin−orbit coupling mixing of the singlet and triplet spin states, did not allow us to follow the complete reaction pathway, we were able to reproduce the structures of the reacting complexes and of the reaction intermediates. The $[(triphosH)Ir(O_2)(catecholate)]^+$ complex is computed to be ∼6 kcal mol^{-1} more stable than the corre-

(25) (a) Allinger, N. L. *J. Am. Chem. Soc.* **1977**, *99*, 8127 and subsequent versions MM2-87, MM2-89, MM2-91. (b) *Hyperchem*, release 3; Hypercube Inc. and Autodesk Inc., 1993.

sponding Co(III) complex, almost independent of the program used to perform the calculations, either ADF or Gaussian98, and independent of the functional applied, either LSDA or GGA (PW91). Also, a qualitative trend between the Mulliken charges computed on the C_1 carbon and the reactivity of the substrate can be obtained from the above calculations. The dioxygenation reaction seems favored if C_1 bears the less positive charge.

We have found that both ADF and Gaussian 98 can accurately describe the geometries of the complexes, while only Gaussian 98 can afford reliable frequencies for the characterization of the computed geometries. ADF, using Slater-type orbitals, seems to afford accurate geometries with smaller basis sets, which can then be used as the initial guess for the Gaussian 98 calculations.

The nice agreement between the computed geometries of the reacting complexes and the adduct with dioxygen encouraged us to pursue applications of this theoretical tool to a more comprehensive investigation of the reaction mechanism, namely, to investigate the influence of the nature of the metal ion on the reaction and to calculate the energetics of the reaction. Inclusion of solvent effects will be also explored in a future work.

Acknowledgment. This work was supported by EC with TMR Contract FMRX-CT980174.

IC990633I